

GPNet: Simplifying Graph Neural Networks via Multi-channel Geometric Polynomials

Xun Liu^{1,2}, Alex Hay-Man Ng^{1,3*}, Fangyuan Lei^{4,5*}, *Member, IEEE*, Yikuan Zhang², Zhengmin Li⁵

¹School of Information Engineering, Guangdong University of Technology

²Department of Electronics, Software Engineering Institute of Guangzhou

³School of Civil and Transportation Engineering, Guangdong University of Technology

⁴Guangdong Provincial Key Laboratory of Intellectual Property and Big Data, Guangdong Polytechnic Normal University

⁵School of Cyber Security, Guangdong Polytechnic Normal University

liuxun.stf@gmail.com hayman.ng@gdut.edu.cn leify@gpnu.edu.cn

zyk@mail.seig.edu.cn lizhengming2004@126.com

Abstract—Graph Neural Networks (GNNs) are a promising deep learning approach for circumventing many real-world problems on graph-structured data. However, these models usually have at least one of four fundamental limitations: over-smoothing, over-fitting, difficult to train, and strong homophily assumption. For example, Simple Graph Convolution (SGC) is known to suffer from the first and fourth limitations. To tackle these limitations, we identify a set of key designs including (D1) dilated convolution, (D2) multi-channel learning, (D3) self-attention score, and (D4) sign factor to boost learning from different types (*i.e.* homophily and heterophily) and scales (*i.e.* small, medium, and large) of networks, and combine them into a graph neural network, GPNet, a simple and efficient one-layer model. We theoretically analyze the model and show that it can approximate various graph filters by adjusting the self-attention score and sign factor. Experiments show that GPNet consistently outperforms baselines in terms of average rank, average accuracy, complexity, and parameters on semi-supervised and full-supervised tasks, and achieves competitive performance compared to state-of-the-art model with inductive learning task.

Index Terms—Graph Neural Network, Graph-structured Data, Arbitrary Graph Filter, Geometric Polynomial



1 INTRODUCTION

MOTIVATED by the excellent performance of Deep Learning (DL) in a wide range of applications, researchers have attempted to generalize DL models to graph-structured data. Their methods are collectively referred to as Graph Neural Networks (GNNs). Recently, GNNs have shown natural advantages on various graph learning tasks, including citation networks [1], [2], [3], traffic forecasting [4], [5], [6], recommendation system [7], [8], social analysis [9], [10], biology [11], [12], drug discovery [13], [14], and computer vision [15], [16]. However, these models have at least one of several fundamental limitations are summarized in the following four-fold.

Limitation 1 *Over-smoothing*. The convolution in many GNNs such as Graph Convolution Network (GCN) [1] is essentially a special form of Laplacian smoothing [17]. The smoothing operation obtains the smoothing node representations of a node and its close neighbors, thus making the features of nodes in the same cluster similar. By applying the smoothing operation repeatedly (stacking many layers, deep GNNs), the features of nodes in same connected component converge to the fixed value and are difficult to distinguish [17], [18]. This is the well-known problem of over-smoothing in GNNs. Residual connection [19] is an effective technology of training very deep neural networks. However, applying the residual connection in GNNs merely slows down the over-smoothing [1]. The classification performance of

these GNNs drops as the number of layers increases (exceed two layers).

Limitation 2 *Over-fitting*. Several methods try to address the over-smoothing of deep GNNs with their redefined convolutions. Xu *et al.* [20] use dense jump connections to flexibly leverage the features of various neighbors for each node. DropEdge [21] randomly deletes a few edges from the input graph to relieve the concerns of over-smoothing. GCNII [22] suggests that GNNs can be generalized to a deep model with the two techniques of initial residual and identity mapping. While these models widen the receptive field of GNNs by increasing the number of network layers, training such models on small graphs may suffer from over-fitting due to the increased substantial parameters to construct these deep GNNs.

Limitation 3 *Difficult to train*. To avoid the over-fitting, more training data and computational resources are required while keeping these models unchanged, which makes it difficult to train on large-scale graphs.

Limitation 4 *Strong homophily assumption*. The convolution of most GNNs such as GCN and Simple Graph Convolution (SGC) [23] can be viewed as a special form of non-negative low-pass filter, which is the key to the success of these models for homophily datasets (similar nodes tend to connect with each other). However, the filter filters out the high-frequency signals of node features, thus being distant from optimal with heterophily datasets (Connected nodes usually belong to different classes). In

*Equal corresponding author

other word, the low-frequency and high-frequency signals of the original features may be optimal for homophily and heterophily graphs, respectively. These observations are highlighted by [24], [25].

A recent work tends to simplify GCN. Wu *et al.* [23] propose SGC, an extremely efficient one-layer model, with competitive performance to GCN in various graph learning tasks, by repeatedly removing the nonlinearities between GCN layers and precomputing the fixed feature extraction. This implies that most classifiers in a wide range of applications are linear. Benefit from the design, SGC has an optimal speed and almost no the concerns of overfitting, due to the single-layer framework and fixed feature extraction. Nevertheless, SGC suffers from the over-smoothing when capturing the features of neighboring nodes at long distances [26]. In addition, SGC assumes strong homophily and may perform worse with heterophily datasets. Therefore, we require a model to tackle these limitations of SGC. If these limitations can be solved while retaining the advantages, the four fundamental problems of current GNN models are addressed naturally.

In this work, we propose Graph Neural Network via Multi-channel Geometric Polynomials (GPNet), a novel simple and efficient one-layer model that aims to learn to fit a distribution under optimal calculations and parameters on homophily and heterophily datasets (Figure 1). From the one-layer design, GPNet has no concerns of overfitting and difficulty training on graphs (address limitations 2 and 3). GPNet can be viewed as a graph analogue of dilated convolution [27], which allows for enlarging the receptive field without loss of resolution by applying a dilation factor. In GPNet, we propose to combine the multi-channel geometric polynomials of the normalized adjacency matrices (with or without self-loops) of various dilation factors to increase the receptive field without bringing over-smoothing (address limitation 1). The main challenge is how to use signals of different frequencies to adapt to different types of networks. To tackle the challenge, we design the two simple techniques of self-attention score and sign factor to achieve performance improvement for both heterophily and homophily (address limitation 4). Theoretical analysis shows that GPNet can fit different types of filters via the adjustment of the self-attention score and sign factor to adapt to both homophily and heterophily networks. We summarize the main contributions as follows:

Key Designs in Both Homophily and Heterophily. We provide several key designs to generalize GNNs to heterophily settings without trading off accuracy in homophily: (D1) dilated convolution, (D2) multi-channel learning, (D3) self-attention score, and (D4) sign factor.

GPNet Framework. We propose GPNet, a simple and efficient one-layer model that learns graph representations for different types of networks in an end-to-end fashion, to tackle the four fundamental limitations of GNNs.

Comprehensive Evaluation. Extensive experiments on ten real-world networks demonstrate that GPNet achieves better accuracy with similar complexity and parameters over SGC, and compares favorably against other baselines in terms of classification accuracy, parameters, and complexity on both homophily and heterophily graphs.

The rest of the paper is organized as follows. In Section 2, we briefly introduce relevant GNN literature. We propose our key designs and GPNet architecture in Section 3. Section 4 presents the analysis of SGC, the proposed GPNet, and relation between GPNet and representative models. In Section 5, we evaluate the

performance of GPNet on various graph learning tasks. Section 6 summarizes the paper.

2 RELATED WORK

Motivated by the limited learning ability of Convolution Neural Networks (CNNs) for dealing with non-Euclidean applications, Spectral CNN [28] and ChebyShev [29] use graph signal theory to first extend CNNs on graphs. Kipf and Welling [1] propose GCN by simplifying the Chebyshev polynomials of [29]. Li *et al.* [17] point out that each convolution of GCN is essentially equivalent to an operation of Laplacian smoothing, which brings the concerns of over-smoothing when repeatedly applying the operation. Many GNNs are generally shallow [30] due to the over-smoothing. This shallow naturally limits the learning ability of obtaining the features of neighboring nodes at different distances. Several works design deep GNNs to improve the learning ability of graph representation. Li *et al.* [31] apply the concepts of CNNs to construct a 56-layer GNN. Xu *et al.* [20] propose three models of jumping knowledge (JK) networks based on three aggregation schemes of concatenation, max-pooling, and LSTM-attention to adjust the range of information aggregated by each node according to different positions and structures of the graph. Rong *et al.* [21] propose the DropEdge architecture to relieve the concerns of overfitting and over-smoothing in deep GNNs. By designing the two effective techniques of identity mapping and initial residual, Chen *et al.* [22] propose Graph Convolutional Network via Initial Residual and Identity Mapping (GCNII) to achieve better performance compared to baselines on various semi-supervised and full-supervised tasks. Several researches devote to leverage the information based on sampling to improve the scalability of GNNs [9], [32], [33], [34]. Graph attentional models suggest adjusting edge weights at each layer to improve the expressive power of learning graph representations on various graph learning tasks [2], [35], [36], [37], [38]. Several works directly capture the multi-hop neighborhood information of nodes through higher-order graph convolution [3], [39], [40], [41], [42], [43] instead of traditional convolutions with stacked layers.

Recently, researchers have focused on simpler and efficient models to significantly reduce training time in downstream applications. Thekumparampil *et al.* [35] design a linear GNN model that removes all intermediate non-linear activation functions to simplify computations. SGC [23] achieves comparable performance under optimal speed and parameters to GCN by removing the nonlinearities between GCN layers and collapsing the weight matrices between consecutive layers. gfNN [44] addresses the limitation that SGC and GCN may work worse in two cases of noisy features and nonlinear features spaces, while retaining the speed of SGC.

Nevertheless, most of the GNN models mentioned above are designed only for homophily datasets, which may not work well on heterophily datasets. Geom-GCN [45], H₂GCN [24], FAGCN [46], TDGNN [47], GPRGNN [48], and CPGNN [25] that are explicitly designed to perform well on heterophily graphs. However, these models need to be improved in terms of efficiency, test accuracy, and parameters, and may fail to work on large-scale graphs.

3 METHODOLOGY

3.1 Preliminaries

Notations. We follow [1] to describe an undirected graph $\mathcal{G} = (\mathcal{V}, \mathcal{E}, X, A)$ with e edges and n nodes (vertices), where \mathcal{E} and \mathcal{V} denote the edge set and node set respectively, $X \in R^{n \times d}$ is the initial feature matrix for all nodes of \mathcal{G} assuming each node has d features, and $A \in \{0, 1\}^{n \times n}$ is the adjacency matrix with each entry $a_{km} = 1$ if there exists an edge (directly connected) between vertex v_k and v_m , otherwise $a_{km} = 0$. We can utilize an identity matrix I to add the self-loops of \mathcal{G} . Most of GNN models leverage an adjacency matrix with self-loops \tilde{A} to describe the edge relationships of \mathcal{G} , with $\tilde{A} = A + I$. The graph Laplacian matrix is defined as $L = D - A$, where D is the degree matrix of \mathcal{G} . Its normalized version $L_{sym} = D^{-\frac{1}{2}} L D^{-\frac{1}{2}}$ is a symmetric positive semidefinite matrix with eigendecomposition $L = U \Lambda U^T$, where U is orthonormal eigenvectors and $L = \Lambda = \text{diag}(\lambda_1, \dots, \lambda_n)$ denotes a diagonal matrix of eigenvalues $\lambda_1, \dots, \lambda_n$.

Graph Convolution Network. As described in GCN [1], each convolution in GCN updates node representations by capturing information from neighbors, which includes three stages: feature propagation, linear transformation, and nonlinear activation.

Feature propagation is the unique mechanism of aggregating information from neighbors in GCN compared to Multi-layer Perceptron (MLP). We can write the mechanism in sparse matrix form as:

$$\hat{H}^{(l)} \leftarrow S_{sym} H^{(l)}, \quad (1)$$

where $H^{(l)}$ denotes the input node representations at layer l with $H^{(l)} = X$ if $l = 1$. We use S_{sym} (a symmetric normalized adjacency matrix with added self-loops, with $S_{sym} = \tilde{D}^{-\frac{1}{2}} \tilde{A} \tilde{D}^{-\frac{1}{2}}$) to smooth the node representations locally along the edges between nodes. Here \tilde{D} is the degree matrix of \tilde{A} .

Linear transformation and nonlinear activation. After the feature propagation, the smoothed representations are transformed linearly via a learned weight matrix $\theta^{(l)}$. Finally, a nonlinear activation function ReLU is widely used in GNNs to achieve the pointwise nonlinear transformation of the l -th layer.

$$H^{(l+1)} \leftarrow \text{ReLU}(\hat{H}^{(l)} \theta^{(l)}). \quad (2)$$

Based on Equations (1)-(2), we can write the following Equation for the convolution of GCN.

$$H^{(l+1)} \leftarrow \text{ReLU}(S_{sym} H^{(l)} \theta^{(l)}). \quad (3)$$

By stacking the convolution twice and using a softmax classifier in the last layer to predict labels, we can write a classic 2-layer GCN:

$$Y_{GCN} = \text{softmax}(S_{sym} \text{ReLU}(S_{sym} X \theta^{(1)}) \theta^{(2)}), \quad (4)$$

where $\theta^{(1)}$ and $\theta^{(2)}$ are different weight matrices.

Simple graph convolution. By applying GCN layers repeatedly, we scale GCN to a k -layer architecture.

$$\hat{Y} = \text{softmax}(S_{sym}(\dots \text{ReLU}(S_{sym} X \theta^{(1)}) \dots) \theta^{(k)}). \quad (5)$$

Suppose the nonlinearity between GCN layers is not critical to performance improvement. Therefore, for k -layer GCN, we delete all ReLU functions in the same way as [23]. The k -layer GCN is:

$$\hat{Y} = \text{softmax}(S_{sym}(\dots (S_{sym} X \theta^{(1)}) \dots) \theta^{(k)}). \quad (6)$$

By collapsing the repeated multiplication with the S_{sym} into a single matrix S_{sym}^k and letting $\theta = \theta^{(1)} \dots \theta^{(k)}$ to simplify the parameters and calculations, the model becomes:

$$\hat{Y}_{SGC} = \text{softmax}(S_{sym}^k X \theta), \quad (7)$$

which is called Simple Graph Convolution (SGC) [23].

3.2 Key Designs

In this section, we propose four key designs that help improve the performance of learning from different types (homophily and heterophily) and scales (small, medium, and large) of networks: (D1) dilated convolution, (D2) multi-channel learning, (D3) self-attention score, and (D4) sign factor. For the sake of clarity, we describe each design in detail.

(D1) Dilated convolution. To enlarge the receptive field without loss of resolution, Yu *et al.* [27] propose a dilated convolution as an alternative to stacking consecutive pooling layers. Their experiments on semantic segmentation tasks demonstrate the effectiveness of the convolution for performance improvement. We suppose that dilation also helps improve the performance of GNNs on graph learning tasks. Therefore, we introduce dilated convolution to GNNs. There are many possible ways to construct a dilated neighborhood. We find a set of neighboring nodes at different distances by applying the power of adjacency matrix (with or without self-loops) to construct geometric dilated neighborhoods. We define the geometric dilated neighborhoods by taking the adjacency matrix with self-loops as an example.

$$f_d^{(m)} = \{\hat{A}^{d_m+q_0}, \hat{A}^{q_m+d_m+q_0}, \dots, \hat{A}^{(k-1)q_m+d_m+q_0}\}, \quad (8)$$

where $d_m + q_0, q_m + d_m + q_0, \dots, (k-1)q_m + d_m + q_0$ are a set of dilation factors and $\hat{A}^{(k-1)q_m+d_m+q_0}$ denotes the $(k-1)q_m + d_m + q_0$ power of \hat{A} . Figure 2 provides two ways to construct our geometric dilated neighborhoods. With the dilated neighborhoods, we define our geometric dilated convolution.

$$H_d^{(m)} = \text{AGGR}\{\hat{A}^{d_m+q_0}, \hat{A}^{q_m+d_m+q_0}, \dots, \hat{A}^{(k-1)q_m+d_m+q_0}\} X W, \quad (9)$$

where AGGR is an aggregation function that aggregates representations from the dilated neighborhoods in sum way, and W denotes a learned weight matrix.

(D2) Multi-channel learning. In Equation (9), the single-channel convolution can effectively learn the interaction of neighboring nodes with different dilation factors. To further improve the interaction, we introduce multi-channel learning to our geometric dilated convolution.

$$H_d = \text{aggregate}(H_d^{(1)}, \dots, H_d^{(m)}), \quad (10)$$

where $H_d^{(m)}$ is the geometric dilated convolution of the m -th channel, and *aggregate* is an aggregation function that brings no extra parameters and is described in detail in Section 3.4.

(D3) Self-attention score. To analyze the contribution of the features of self-node to performance improvement compared to the features of its neighboring nodes, we introduce a self-attention score $\alpha \in R$ into the proposed model.

$$H_{0d}^{(m)} = \text{AGGR}(\alpha \hat{A}^0 X W, H_d^{(m)}). \quad (11)$$

We set the hyperparameter α , which will be discussed in Section 5.7, according to different types and scales of networks. By setting $\alpha > 0$, the final representation of each node consists of at least a fraction of X .

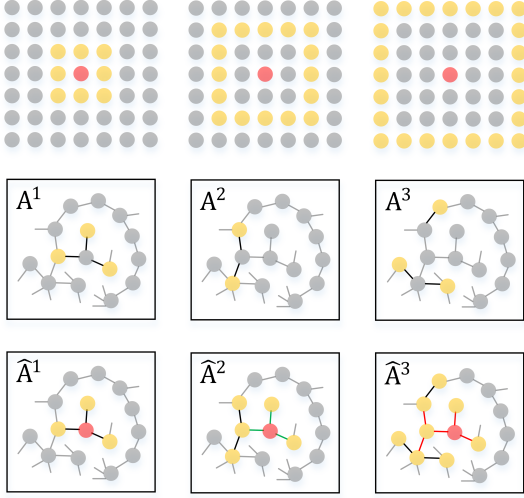


Fig. 2. **Geometric dilated neighborhoods.** Visualization of dilated neighborhoods on a 2D image and on a graph. (top) 2D neighborhoods with kernel size 3 and dilation factor 1, 2, 3 (left to right). (middle) Geometric dilated neighborhoods with dilation factor 1, 2, 3 (left to right). (bottom) Geometric dilated neighborhoods with self-loops and dilation factor 1, 2, 3 (left to right).

where β is a key another hyperparameter that controls the type of filter along with α . We set $\beta = 1$ and $\beta = -1$ for homophily and heterophily networks in most cases, respectively. If the effect of W is ignored, the filter with $\beta = 1$ mainly considers the low-frequency components while the filter with $\beta = -1$ pays more attention to the high-frequency components (see Theorem 3).

Summary of designs. To sum up, we believe that the first two designs are key techniques for boosting the performance of learning graph representations, and the latter two designs are effective strategies for fitting different types and scales of networks.

3.3 The Overall Architecture

Current GNNs suffer from at least one of the fundamental limitations including over-smoothing, over-fitting, difficulty training, and strong homophily assumption. SGC, as an extremely efficient one-layer model, addresses the problems of over-fitting and difficulty training, by removing the nonlinearities between GCN layers and precomputing the fixed feature extraction [23]. However, the analysis in Section 4.1 shows that SGC fails to tackle the over-smoothing and is distant from optimal with heterophily graphs. To tackle the limitations, we propose a new simple and efficient one-layer model called GPNet. In GPNet, we provide the four key designs to fit a distribution under optimal complexity and accuracy for different types and scales of networks. With the designs, we design a simple convolution model with multi-channel geometric polynomials to learn graph representations. In output layer, we apply a softmax classifier to classify each node.

3.4 Simple Convolution with Multi-channel Geometric Polynomials

Our simple convolution with multi-channel geometric polynomials to update node representations in three stages, *i.e.* geometric adjacency matrix, geometric feature propagation, and geometric linear transformation.

Geometric adjacency matrix. In GCNs, we use S_{sym} to obtain the features of a node and its first-order neighboring nodes.

However, S_{sym} fails to obtain the features of high-order neighboring nodes. In SGC, we apply the k power of S_{sym} (S_{sym}^k) in an one-layer model to capture the features of neighboring nodes that are k -hops away. As shown in Section 4.1, SGC has difficulty in capturing the features of neighboring nodes at long distances and fails to fit well a distribution with heterophily. To tackle the problems, we combine various geometric powers of the normalized adjacency matrix (with or without self-loops) based on different dilation factors into a single geometric adjacency matrix with six stages: (S1) features obtaining of own node and its neighboring nodes; (S2) features summation of neighboring nodes; (S3) features self-attention of own node; (S4) features sign of neighboring nodes; (S5) features summation of S3 and S4; and (S6) features aggregation. In the geometric adjacency matrix, we take the normalized adjacency matrix with self-loops \hat{A} as an example to facilitate the analysis of the designed model.

(S1) Features obtaining of own node and its neighboring nodes. With different dilation factors, we obtain the features of own node and its neighboring nodes at various distances via a series of functions of \hat{A} .

$$f(\hat{A}) = (f_1(\hat{A}), f_2(\hat{A}), \dots, f_m(\hat{A})), \quad (13)$$

where $f_m(\hat{A})$ is the geometric polynomial of \hat{A} for $i \neq 0$, which is defined as:

$$f_m(\hat{A}) = \begin{cases} \hat{A}^i, & i = 0 \\ \hat{A}^{(i-1)q_m + d_m + q_0}, & i = 1, 2, \dots, k \end{cases} \quad (14)$$

where m and k are the number of channels and the number of terms, respectively. Here $q_0 \geq 0$, $q_m \geq 1$, and $d_m \geq 0$ are the first item coefficient, common ratios, and neighborhood coefficients of $f_m(\hat{A})$, respectively. In Equation (14), we can fix the value of m to obtain the geometric adjacency matrices of different dilation factors. For example when $m = 1$, we can get a set of adjacency matrices with dilation factor $d_1 + q_0, q_1 + d_1 + q_0, \dots, (k-1)q_1 + d_1 + q_0$.

(S2) Features summation of neighboring nodes. After the stage S1, we sum the features of neighboring nodes using the geometric polynomials of adjacency matrices with various dilation factors.

$$\begin{aligned} f_1(\hat{A})_{sum} &= \hat{A}^{d_1 + q_0} + \hat{A}^{q_1 + d_1 + q_0} + \dots + \hat{A}^{(k-1)q_1 + d_1 + q_0}, \\ f_2(\hat{A})_{sum} &= \hat{A}^{d_2 + q_0} + \hat{A}^{q_2 + d_2 + q_0} + \dots + \hat{A}^{(k-1)q_2 + d_2 + q_0}, \\ &\vdots \\ f_m(\hat{A})_{sum} &= \hat{A}^{d_m + q_0} + \hat{A}^{q_m + d_m + q_0} + \dots + \hat{A}^{(k-1)q_m + d_m + q_0}. \end{aligned} \quad (15)$$

(S3) Features self-attention of own node. We apply a self-attention score $\alpha \in R$ to adjust the contribution of node's own features.

$$S^0 = \alpha \hat{A}^0. \quad (16)$$

(S4) Features sign of neighboring nodes. We propose a sign factor β ($\beta = 1$ or -1) that is a key design of fitting a distribution on both homophily and heterophily graphs. By applying β to Equation (16), we have:

$$\begin{aligned} \beta f_1(\hat{A})_{sum} &= \beta \left(\hat{A}^{d_1 + q_0} + \hat{A}^{q_1 + d_1 + q_0} + \dots + \hat{A}^{(k-1)q_1 + d_1 + q_0} \right), \\ \beta f_2(\hat{A})_{sum} &= \beta \left(\hat{A}^{d_2 + q_0} + \hat{A}^{q_2 + d_2 + q_0} + \dots + \hat{A}^{(k-1)q_2 + d_2 + q_0} \right), \\ &\vdots \\ \beta f_m(\hat{A})_{sum} &= \beta \left(\hat{A}^{d_m + q_0} + \hat{A}^{q_m + d_m + q_0} + \dots + \hat{A}^{(k-1)q_m + d_m + q_0} \right). \end{aligned} \quad (17)$$

(S5) Features summation of S3 and S4. After the stages of S3 and S4, we sum the features of S3 and S4 in Equation (18).

$$\begin{aligned}
g_1(\hat{A})_{sum} &= S^0 + \beta f_1(\hat{A})_{sum} \\
&= \alpha \hat{A}^0 + \beta (\hat{A}^{d_1+q_0} + \hat{A}^{q_1+d_1+q_0} + \dots + \hat{A}^{(k-1)q_1+d_1+q_0}), \\
g_2(\hat{A})_{sum} &= S^0 + \beta f_2(\hat{A})_{sum} \\
&= \alpha \hat{A}^0 + \beta (\hat{A}^{d_2+q_0} + \hat{A}^{q_2+d_2+q_0} + \dots + \hat{A}^{(k-1)q_2+d_2+q_0}), \\
&\vdots \\
g_m(\hat{A})_{sum} &= S^0 + \beta f_m(\hat{A})_{sum} \\
&= \alpha \hat{A}^0 + \beta (\hat{A}^{d_m+q_0} + \hat{A}^{q_m+d_m+q_0} + \dots + \hat{A}^{(k-1)q_m+d_m+q_0}). \tag{18}
\end{aligned}$$

(S6) Features aggregation. Finally, we aggregate the features of $g_1(\hat{A})_{sum}, g_2(\hat{A})_{sum}, \dots, g_m(\hat{A})_{sum}$.

$$\hat{S}_{adj} = aggregate(g_1(\hat{A})_{sum}, g_2(\hat{A})_{sum}, \dots, g_m(\hat{A})_{sum}), \tag{19}$$

where *aggregate* is an aggregation function. Instead of the aggregation schemes of increasing parameters as in concatenation and LSTM-attention [20], we explore four aggregation approaches without additional parameters, including Max-FP, Min-FP, Avg-FP, and Sum-FP. Our aggregation approaches are all element-wise operations, which are defined as:

$$\begin{aligned}
\hat{S}_{adj} &= \text{Max-FP}(g_1(\hat{A})_{sum}, g_2(\hat{A})_{sum}, \dots, g_m(\hat{A})_{sum}) \\
&= \max(g_1(\hat{A})_{sum}, g_2(\hat{A})_{sum}, \dots, g_m(\hat{A})_{sum}), \tag{20}
\end{aligned}$$

$$\begin{aligned}
\hat{S}_{adj} &= \text{Min-FP}(g_1(\hat{A})_{sum}, g_2(\hat{A})_{sum}, \dots, g_m(\hat{A})_{sum}) \\
&= \min(g_1(\hat{A})_{sum}, g_2(\hat{A})_{sum}, \dots, g_m(\hat{A})_{sum}), \tag{21}
\end{aligned}$$

$$\begin{aligned}
\hat{S}_{adj} &= \text{Avg-FP}(g_1(\hat{A})_{sum}, g_2(\hat{A})_{sum}, \dots, g_m(\hat{A})_{sum}) \\
&= \text{avg}(g_1(\hat{A})_{sum}, g_2(\hat{A})_{sum}, \dots, g_m(\hat{A})_{sum}) \tag{22} \\
&= \frac{1}{m} \sum_{r=1}^m g_r(\hat{A})_{sum},
\end{aligned}$$

$$\begin{aligned}
\hat{S}_{adj} &= \text{Sum-FP}(g_1(\hat{A})_{sum}, g_2(\hat{A})_{sum}, \dots, g_m(\hat{A})_{sum}) \\
&= \text{sum}(g_1(\hat{A})_{sum}, g_2(\hat{A})_{sum}, \dots, g_m(\hat{A})_{sum}) \tag{23} \\
&= \sum_{r=1}^m g_r(\hat{A})_{sum}.
\end{aligned}$$

Proposition 1. *Geometric adjacency matrix is an operation of permutation invariance.*

Proof. In Max-FP, Min-FP, Avg-FP, and Sum-FP, we have

$$\begin{aligned}
&\text{Max-FP}(g_1(\hat{A})_{sum}, g_2(\hat{A})_{sum}, \dots, g_m(\hat{A})_{sum}) = \\
&\text{Max-FP}(g_m(\hat{A})_{sum}, g_{m-1}(\hat{A})_{sum}, \dots, g_1(\hat{A})_{sum}),
\end{aligned}$$

$$\begin{aligned}
&\text{Min-FP}(g_1(\hat{A})_{sum}, g_2(\hat{A})_{sum}, \dots, g_m(\hat{A})_{sum}) = \\
&\text{Min-FP}(g_m(\hat{A})_{sum}, g_{m-1}(\hat{A})_{sum}, \dots, g_1(\hat{A})_{sum}),
\end{aligned}$$

$$\begin{aligned}
&\text{Avg-FP}(g_1(\hat{A})_{sum}, g_2(\hat{A})_{sum}, \dots, g_m(\hat{A})_{sum}) = \\
&\text{Avg-FP}(g_m(\hat{A})_{sum}, g_{m-1}(\hat{A})_{sum}, \dots, g_1(\hat{A})_{sum}),
\end{aligned}$$

$$\begin{aligned}
&\text{Sum-FP}(g_1(\hat{A})_{sum}, g_2(\hat{A})_{sum}, \dots, g_m(\hat{A})_{sum}) = \\
&\text{Sum-FP}(g_m(\hat{A})_{sum}, g_{m-1}(\hat{A})_{sum}, \dots, g_1(\hat{A})_{sum}),
\end{aligned}$$

thus finishing the proof. \square

Algorithm 1 Simple convolution with multi-channel geometric polynomials

Inputs: a normalized adjacency matrix with self-loops \hat{A} , an initial feature matrix X , and a learned weight matrix W .

```

1: for  $i = 0$  do
2:    $f_m^{(i)}(\hat{A}) = \hat{A}^i$ .
3: end for
4: for  $i = 1$  to  $k$  do
5:    $f_m^{(i)}(\hat{A}) = \hat{A}^{(i-1)q_m+d_m+q_0}$ .
6: end for
7: Calculate geometric adjacency matrix  $\hat{S}_{adj}$  via the six stages of (S1)-(S6).
8:  $\bar{H} = \hat{S}_{adj} X$ .
9:  $H = \bar{H} W = \hat{S}_{adj} X W$ .
10: return  $H$ 

```

Proposition 2. *Geometric adjacency matrix is an operation of preserving graph topology.*

Proof. Let $\hat{A} \in R^{n \times n}$, then

$$\begin{aligned}
g_1(\hat{A})_{sum} &= \alpha \hat{A}^0 + \beta (\hat{A}^{d_1+q_0} + \hat{A}^{q_1+d_1+q_0} + \dots + \hat{A}^{(k-1)q_1+d_1+q_0}) \in R^{n \times n}, \\
g_2(\hat{A})_{sum} &= \alpha \hat{A}^0 + \beta (\hat{A}^{d_2+q_0} + \hat{A}^{q_2+d_2+q_0} + \dots + \hat{A}^{(k-1)q_2+d_2+q_0}) \in R^{n \times n}, \\
&\vdots \\
g_m(\hat{A})_{sum} &= \alpha \hat{A}^0 + \beta (\hat{A}^{d_m+q_0} + \hat{A}^{q_m+d_m+q_0} + \dots + \hat{A}^{(k-1)q_m+d_m+q_0}) \in R^{n \times n},
\end{aligned}$$

and $\hat{S}_{adj} = aggregate(g_1(\hat{A})_{sum}, g_2(\hat{A})_{sum}, \dots, g_m(\hat{A})_{sum}) \in R^{n \times n}$. Equations (20)-(23) show that the aggregation schemes of Max-FP, Min-FP, Avg-FP, and Sum-FP are element-wise operations. Therefore, the spatial location of \hat{S}_{adj} is the same as that of \hat{A} , which finishes the proof. \square

Geometric feature propagation. Geometric feature propagation is what distinguishes our model from many GNNs such as GCN and SGC. The node feature matrix X is averaged with the features of neighboring nodes constructed by the geometric adjacency matrix.

$$\bar{H} = \hat{S}_{adj} X. \tag{24}$$

This step encourages similar predictions among locally connected nodes on homophily graphs and improves the ability of distinguishing the features of nodes in different clusters on heterophily graphs. In addition, we can think of \bar{H} as a feature pre-processing step before training due to the parameterless computations of \bar{H} .

Geometric linear transformation. After the geometric feature propagation, we implement a geometric linear transformation by $\bar{H}W$.

$$H = \bar{H}W. \tag{25}$$

Based on Equations (24)-(25), we conclude that the proposed simple convolution with multi-channel geometric polynomials takes the following form.

$$H = \hat{S}_{adj} X W. \tag{26}$$

Our algorithm (with self-loops) is summarized in Algorithm 1. Our convolution model aims to fit a distribution on both homophily and heterophily graphs via four designs of (D1)-(D4). In GCN and SGC, the convolution acts as a low-pass filter, which is suitable

for homophily graphs but may not work well with heterophily. However, our convolution adapts to different types of networks by utilizing signals of different frequencies.

3.5 Output Layer

In output layer, we follow Kipf and Welling [1] to predict the label of nodes using a softmax classifier and a cross entropy loss. The output prediction Y_{GPNet} is:

$$Y_{\text{GPNet}} = \text{softmax}(H) = \text{softmax}(\hat{S}_{adj} XW). \quad (27)$$

4 THEORETICAL ANALYSIS

4.1 Analysis of SGC

SGC, as a simplified linear model, has the same increased receptive field of k -layer GNN, which can aggregate the information of neighbor nodes that are k -hops away. We increase the receptive field and aggregate the features of neighbor nodes at more distant distances by taking a larger value of k . However, taking a larger value of k ($k \geq 3$) makes the output features of nodes in the same cluster and different clusters similar and hurts the classification task [26]. This shows that SGC with large k value may suffer from over-smoothing. We propose Theorem 1 for further proof.

Theorem 1. *For an undirected graph, SGC corresponds to a k -step random walk considering self-loops. As k tends to infinity, S_{sym}^k converges to a stationary distribution $\pi = \frac{\tilde{D}}{2e+n}$, where e is the number of edges in the graph.*

Proof. In Equation (7), we have $S_{sym}^k X\theta = (\tilde{D}^{-\frac{1}{2}} \tilde{A} \tilde{D}^{-\frac{1}{2}})^k X\theta$. Let transition matrix with self-loops $\tilde{P} = \tilde{A} \tilde{D}^{-1}$, then

$$\begin{aligned} (\tilde{D}^{-\frac{1}{2}} \tilde{A} \tilde{D}^{-\frac{1}{2}})^k &= \tilde{D}^{-\frac{1}{2}} \tilde{A} \tilde{D}^{-\frac{1}{2}} \cdot \tilde{D}^{-\frac{1}{2}} \tilde{A} \tilde{D}^{-\frac{1}{2}} \cdots \tilde{D}^{-\frac{1}{2}} \tilde{A} \tilde{D}^{-\frac{1}{2}} \\ &= \tilde{D}^{-\frac{1}{2}} (\tilde{A} \tilde{D}^{-1}) (\tilde{A} \tilde{D}^{-1}) \cdots (\tilde{A} \tilde{D}^{-1}) \cdot \tilde{A} \tilde{D}^{-\frac{1}{2}} \\ &= \tilde{D}^{-\frac{1}{2}} (\tilde{A} \tilde{D}^{-1})^{k-1} \cdot \tilde{A} \tilde{D}^{-\frac{1}{2}} \\ &= \tilde{D}^{-\frac{1}{2}} (\tilde{A} \tilde{D}^{-1})^{k-1} \cdot \tilde{A} \tilde{D}^{-\frac{1}{2}} \cdot \tilde{D}^{-\frac{1}{2}} \cdot \tilde{D}^{\frac{1}{2}} \\ &= \tilde{D}^{-\frac{1}{2}} (\tilde{A} \tilde{D}^{-1})^{k-1} \cdot (\tilde{A} \tilde{D}^{-1}) \cdot \tilde{D}^{\frac{1}{2}} \\ &= \tilde{D}^{-\frac{1}{2}} (\tilde{A} \tilde{D}^{-1})^k \tilde{D}^{\frac{1}{2}} \\ &= \tilde{D}^{-\frac{1}{2}} \tilde{P}^k \tilde{D}^{\frac{1}{2}}. \end{aligned} \quad (28)$$

Therefore, S_{sym}^k converges to a stationary distribution $\pi = \frac{\tilde{D}}{2e+n}$ as k goes to infinity. \square

Theorem 1 shows that the distribution is only related to the graph structure while forgetting the initial features, so SGC suffers from over-smoothing under the distribution. In SGC, the convolution corresponds to a fixed non-negative low-pass filter [23] that retains the commonality while ignoring the difference, thus making the learned representations of connected nodes similar. Since the connected nodes of homophily and heterophily graphs usually belong to same cluster and different labels, respectively, SGC is suitable for homophily graphs but may not perform well with heterophily graphs.

Theorem 2. *Many GNNs such as SGC are equivalent to a low-pass filter, and can also be regarded as a high-pass filter.*

Proof. As mentioned in Equation (7), the resulting classifier of SGC is $\hat{Y}_{\text{SGC}} = \text{softmax}(S_{sym}^k X\theta)$, then the propagation matrix

S_{sym}^k corresponds to filter coefficients $\hat{g}(\tilde{\lambda}_i) = (1 - \tilde{\lambda}_i)^k$. Thus, S_{sym}^k acts as a low-pass filter. Let $\theta_{hp} = -\theta$, then $\hat{Y}_{\text{SGC}} = \text{softmax}(-S_{sym}^k X\theta_{hp})$. Therefore, the filter coefficients are $\hat{g}(\tilde{\lambda}_i) = -(1 - \tilde{\lambda}_i)^k$, which can be regarded as a high-pass filter. \square

4.2 Analysis of GPNet

We follow Defferrard *et al.* [29] to introduce the graph convolution between signal x and filter g .

$$g*x = U((U^T g) \odot (U^T x)) = U \text{diag}(\hat{g}_1, \dots, \hat{g}_n) U^T x, \quad (29)$$

where $\text{diag}(\hat{g}_1, \dots, \hat{g}_n)$ denotes a diagonal matrix of spectral filter coefficients. GCN simplifies the graph filter $\text{diag}(\hat{g}_1, \dots, \hat{g}_n)$ as $I - \Lambda$.

In Equation (1), the propagation matrix is $S_{sym} = \tilde{D}^{-\frac{1}{2}} \tilde{A} \tilde{D}^{-\frac{1}{2}}$, then the augmented normalized Laplacian matrix is defined as $\tilde{L}_{sym} = \tilde{D}^{-\frac{1}{2}} (\tilde{D} - \tilde{A}) \tilde{D}^{-\frac{1}{2}} = I - S_{sym}$. Therefore, the filter coefficients are $\hat{g}(\tilde{\lambda}_i) = (1 - \tilde{\lambda}_i)$, where $\tilde{\lambda}_i$ denote the eigenvalues of \tilde{L}_{sym} . In GPNet, the filter coefficients are $\hat{g}(\tilde{\lambda}_i) = \text{aggregate}(\hat{g}_1(\tilde{\lambda}_i), \hat{g}_2(\tilde{\lambda}_i), \dots, \hat{g}_m(\tilde{\lambda}_i))$, where $\hat{g}_m(\tilde{\lambda}_i) = \alpha + \beta((1 - \tilde{\lambda}_i)^{d_m+q_0} + (1 - \tilde{\lambda}_i)^{q_m+d_m+q_0} + \dots + (1 - \tilde{\lambda}_i)^{(k-1)q_m+d_m+q_0})$.

Theorem 3. *GPNet can approximate various graph filters.*

Proof. Let $m = 1$, then the filter coefficients of GPNet are $\hat{g}(\tilde{\lambda}_i) = \alpha + \beta((1 - \tilde{\lambda}_i)^{d_1+q_0} + (1 - \tilde{\lambda}_i)^{q_1+d_1+q_0} + \dots + (1 - \tilde{\lambda}_i)^{(k-1)q_1+d_1+q_0})$. As shown in Section 3.4, we have $q_0 \geq 0, q_1 \geq 1$, and $d_1 \geq 0$. We set $\alpha > 0$ and $\beta = 1$, then the filter coefficients become $\hat{g}(\tilde{\lambda}_i) = \alpha + (1 - \tilde{\lambda}_i)^{d_1+q_0} + (1 - \tilde{\lambda}_i)^{q_1+d_1+q_0} + \dots + (1 - \tilde{\lambda}_i)^{(k-1)q_1+d_1+q_0}$, which acts as a low-pass graph filter. We set $\alpha \geq 0$ and $\beta = -1$, then the filter coefficients are $\hat{g}(\tilde{\lambda}_i) = \alpha - (1 - \tilde{\lambda}_i)^{d_1+q_0} - (1 - \tilde{\lambda}_i)^{q_1+d_1+q_0} - \dots - (1 - \tilde{\lambda}_i)^{(k-1)q_1+d_1+q_0}$, which achieves a high-pass graph filter. We set $\alpha \geq 0, \beta = 1, k = 1, d_1 = 0$, and $q_0 = 0$, then the filter coefficients become $\hat{g}(\tilde{\lambda}_i) = \alpha + 1$, *i.e.* an all-pass graph filter. \square

Theorem 3 shows that GPNet can pay attention to signals of different frequencies to fit different types of networks.

GPNet without over-smoothing. Equations (18), (19), and (24) suggest that the proposed geometric feature propagation carries the features from both input node and its nodes of geometric dilated neighborhoods by setting $\alpha > 0$. This ensures that GPNet can prevent the over-smoothing even if the number of terms goes to infinity. More precisely, when $\alpha = 0$, the feature propagation considers the features of these neighboring nodes $d_m + q_0, q_m + d_m + q_0, \dots, (k-1)q_m + d_m + q_0$. Even if k tends to infinity, the feature propagation always includes the features that are $d_m + q_0$ hops away. Similarly, the feature propagation always includes the features of input node and its neighboring nodes that are $d_m + q_0$ hops away when $\alpha > 0$. Therefore, our GPNet can avoid the over-smoothing even with k going to infinity.

4.3 Analysis of Relation between GPNet and Representative Models

Relation of GPNet and SGC. SGC with 2-hops is:

$$Y_{\text{SGC}} = \text{softmax}(S_{sym}^2 X\theta). \quad (30)$$

TABLE 1
Dataset statistics. Net. denotes Network.

Dataset	Cora	Citeseer	Pubmed	Reddit	Cornell	Texas	Wisconsin	Chameleon	Squirrel
Nodes	2,708	3,327	19,717	233K	183	183	251	2,277	5,201
Features	1,433	3,703	500	602	1,703	1,703	1,703	2,325	2,089
Classes	7	6	3	41	5	5	5	5	5
Edges	5,429	4,732	44,338	11.6M	295	309	499	36,101	198K
Network Type	Homophily Citation Net.	Homophily Citation Net.	Homophily Citation Net.	Homophily Social Net.	Heterophily Webpage Net.	Heterophily Webpage Net.	Heterophily Wikipedia Net.	Heterophily Wikipedia Net.	Heterophily Wikipedia Net.

In GPNet, let $\alpha = 0$, $\beta = 1$, $k = 1$, and $d_1 + q_0 = 2$, then $\hat{S}_{adj} = g_1(\hat{A})_{sum} = \hat{A}^2$. Thus the model becomes:

$$Y_{\text{GPNet}} = \text{softmax}(\hat{A}^2 X W). \quad (31)$$

As \hat{A} and W are the augmented normalized adjacency matrix and trainable weight matrix respectively equivalent to S_{sym} and θ in Equation (30). Therefore, SGC can be reduced to a special case of GPNet.

Relation of GPNet and gfNN. In gfNN [44], the output prediction Y_{gfNN} is:

$$Y_{\text{gfNN}} = \text{softmax}(\sigma(\hat{A}^2 X W_1) W_2), \quad (32)$$

where σ is an activation function, W_1 and W_2 are different weight matrices. If we remove the activation function or use an identity activation function, then Y_{gfNN} becomes:

$$Y_{\text{gfNN}} = \text{softmax}(\hat{A}^2 X W_1 W_2). \quad (33)$$

Let $W = W_1 W_2$, then gfNN can be regarded as a special case of GPNet.

Relation of GPNet and MLP. In GPNet, let $m = 1$, $k = 1$, $d_1 = 0$, and $q_0 = 0$, then $\hat{S}_{adj} = g_1(\hat{A})_{sum} = (\alpha + \beta)\hat{A}^0$. By $W_{mlp} = (\alpha + \beta)W$, the model takes the following form:

$$Y_{\text{GPNet}} = \text{softmax}((\alpha + \beta)\hat{A}^0 X W) = \text{softmax}(X W_{mlp}). \quad (34)$$

Thus, MLP with a layer can be regarded as a special case of GPNet.

4.4 Analysis of Time Complexity and Parameters

As described in Section 3.4, the computation of $\bar{H} = \hat{S}_{adj} X$ (geometric feature propagation) requires no weight. Therefore, by precomputing a parameter-free feature extraction \bar{H} , the entire training time and parameters of GPNet are the same as a particularly efficient SGC.

5 EXPERIMENTS

We evaluate the performance of GPNet against the competitors, with the goal of answering the following research questions:

Q1 Can GPNet tackle the over-smoothing when obtaining the features of neighboring nodes with large k-hops?

Q2 Can GPNet perform well on heterophily graphs without trading off accuracy in homophily?

Q3 Can GPNet work well on large-scale graphs when many GNNs fail to deal with such data?

Q4 How does GPNet compare to the state-of-the-art (SOTA) models for different types of networks?

Q5 How does GPNet compare to baselines in terms of the complexity and parameters?

5.1 Dataset

We evaluate the performance of GPNet against the competitors on multiple real-world datasets chosen from benchmarks commonly used on node classification tasks. More specifically, for semi-supervised node classification, we use three homophilic datasets Cora, Citeseer, and Pubmed [49] on public splits [1]. For full-supervised node classification, we also use the three homophilic datasets and five heterophily datasets including webpage graphs Cornell, Texas, and Wisconsin [45], and Wikipedia graphs Chameleon and Squirrel [50]. For these datasets of the full-supervised node classification tasks, we follow Pei *et al.* [45] to split the nodes of training, validation and testing. For inductive learning, we include a large graph Reddit [32]. We summarize the statistics of these datasets in Table 1.

TABLE 2
The classification performance (%) over the methods on semi-supervised node classification tasks. Avg. R. denotes Average Rank.

Method	Pubmed	Citeseer	Cora	Avg. R.	Average
GCN	79.0	70.3	81.5	9.83	76.9
GAT	79.0±0.3	72.5±0.7	83.0±0.7	7.67	78.2
SGC	78.9±0.0	71.9±0.1	81.0±0.0	10.17	77.3
MixHop-learn	80.8±0.6	71.4±0.8	81.9±0.4	7	78.0
APPNP	80.1	71.8	83.3	6.5	78.4
ARMA	78.9	72.5	83.4	7.33	78.3
IncepGCN+DropEdge	79.5	72.7	83.5	4.17	78.6
JKNet	78.1	69.8	81.1	11.67	76.3
JKNet+DropEdge	79.2	72.6	83.3	6.17	78.4
GCNII	80.2±0.4	73.4±0.6	85.5±0.5	2	79.7
FAGCN	79.4±0.3	72.7±0.8	84.1±0.5	4.17	78.7
GPNet (ours)	81.5±0.0	74.8±0.1	84.6±0.1	1.33	80.3

5.2 Model Configurations

We implement our proposed GPNet using Adam [51] optimizer in Pytorch [52]. We now report the search space of hyperparameters that are optimized repeatedly on each dataset. The learning rate is searched from $\{0.0003, 0.01, 0.05, 0.1\}$, the dropout is searched from $\{0, 0.1, 0.3, 0.8, 0.95\}$, the L_2 regularization factor is searched from $\{1e^{-10}, 1e^{-7}, 7e^{-6}, 5e^{-5}, 6e^{-5}, 1e^{-4}, 2e^{-4}, 5e^{-4}, 6e^{-3}\}$, the training epochs are searched from 700, 800, 1,000, 1,200, 2,000, 2,200, 5,000, 7,000, 50,000, the k is searched from $\{2, 3, 4, 5, 7, 8, 9, 13\}$, the m is searched from $\{2, 3\}$, the q_1 is searched from $\{2, 4, 5\}$, the q_2 is searched from $\{2, 5, 6\}$, the d_2 is searched from $\{1, 3\}$, the d_3 is searched from $\{6, 9\}$, and the aggregation function is searched from Max-FP, Min-FP, Avg-FP, Sum-FP. The d_1 , q_0 and q_3 are set to 0, 1 and 6, respectively. We set the self-attention score α based on different types of networks, with $\alpha = 1$ on citation networks, with $\alpha = 0$ on Wikipedia networks, with $\alpha = 20, \alpha = 19, \alpha = 70$ on Cornell, Texas, and Wisconsin, and with $\alpha = 0.2$ on Reddit. We set the sign factor

TABLE 3

The classification performance (%) over the methods on full-supervised node classification tasks. Avg. R. denotes Average Rank.

Method	Chameleon	Squirrel	Wisconsin	Cornell	Texas	Pubmed	Citeseer	Cora	Avg. R.	Average
MLP	46.21±3.0	28.77±1.6	85.29±3.3	81.89±6.4	80.81±4.8	87.16±0.4	74.02±1.9	75.69±2.0	14.13	69.98
GCN	64.82±2.2	53.43±2.0	51.76±3.1	60.54±5.3	55.14±5.2	88.42±0.5	76.50±1.4	86.98±1.3	12.88	67.20
GAT	60.26±2.5	40.72±1.6	49.41±4.1	61.89±5.1	52.16±6.6	86.33±0.5	76.55±1.2	87.30±1.1	14.25	64.33
SGC	33.70±3.5	46.90±1.7	53.49±5.1	58.68±3.8	60.43±5.1	85.11±0.5	76.01±1.8	87.07±1.2	15.50	62.67
MixHop	60.50±2.5	43.80±1.5	75.88±4.9	73.51±6.3	77.84±7.7	85.31±0.6	76.26±1.3	87.61±0.9	12.38	72.59
APPNP	47.50±1.8	33.51±2.0	81.42±4.3	77.02±7.0	78.37±6.0	87.94±0.6	77.06±1.7	87.71±1.3	11.75	71.32
Geom-GCN	60.9	38.14	64.12	60.81	67.57	90.05	77.99	85.27	11.38	68.11
H ₂ GCN	60.11±2.2	36.48±1.9	87.65±5.0	82.70±5.3	84.86±7.2	89.49±0.4	77.11±1.6	87.87±1.2	7.69	75.78
FAGCN	56.31±3.2	42.43±2.1	81.56±4.6	76.12±7.7	78.11±5.0	85.74±0.4	74.86±2.4	83.21±2.0	13.88	72.29
LINKX	68.42±1.4	61.81±1.8	75.49±5.7	77.84±5.8	74.60±8.4	87.86±0.8	73.19±1.0	84.64±1.1	12	75.48
GPRGNN	46.58±1.7	31.61±1.2	82.94±4.2	80.27±8.1	78.38±4.4	87.54±0.4	77.13±1.7	87.95±1.2	10.94	71.55
GGCN	71.14±1.8	55.17±1.6	86.86±3.3	85.68±6.6	84.86±4.6	89.15±0.4	77.14±1.5	87.95±1.1	5.50	79.74
GCNII	63.86±3.0	38.47±1.6	80.39±3.4	77.86±3.8	77.57±3.8	90.15±0.4	77.33±1.5	88.37±1.3	7.75	74.25
DeepGCNs	48.75±2.6	31.23±1.4	72.75±4.8	68.38±5.9	70.27±7.1	88.80±0.4	75.58±1.2	85.61±1.9	14.75	67.67
UDGNN _{GCN}	74.53±1.2	68.13±2.6	87.64±3.7	84.32±7.3	84.60±5.3	89.85±0.4	76.05±1.8	86.97±1.2	5.75	81.51
Conn-NSD	65.21±2.0	45.19±1.6	88.73±4.5	85.95±7.7	86.16±2.2	89.28±0.4	75.61±1.9	83.74±2.2	7.31	77.48
GloGNN	69.78±2.4	57.54±1.4	87.06±3.5	83.51±4.3	84.32±4.2	89.62±0.4	77.41±1.7	88.31±1.1	4.63	79.69
GloGNN++	71.21±1.8	57.88±1.8	88.04±3.2	85.95±5.1	84.05±4.9	89.24±0.4	77.22±1.8	88.33±1.1	3.81	80.24
GPNet (ours)	78.61±0.2	71.57±0.1	87.45±0.0	84.10±0.1	87.84±0.0	89.18±0.0	77.20±0.1	88.21±0.1	3.75	83.02

TABLE 4

The test F1-micro score (%) over the methods on Reddit. OOM denotes out of memory.

Method	Reddit
SAGE-GCN	93.0
SAGE-LSTM	95.4
SAGE-mean	95.0
FastGCN	93.7
GaAN	96.4
DGI	94.0
SGC	94.9
GCN	OOM
GAT	OOM
GCNII	OOM
GPRGNN	OOM
GPNet (ours)	95.8 ± 0.0

$\beta = -1$ on Texas and Wisconsin and $\beta = 1$ on other datasets. All results of the proposed methods are averaged over 10 runs with random weight initializations.

5.3 Baselines

Semi-supervised node classification. For the semi-supervised node classification tasks, we compare our method with the following baselines: (1) shallow GNNs: GCN [1], GAT [2], SGC [23], MixHop-learn [3], APPNP [18], and ARMA [43]; (2) deep GNNs: JKNet [20], GCNII [22], and FAGCN [46]. Furthermore, we follow Rong *et al.* [21] to equip DropEdge [21] on two backbones: IncepGCN [21] and JKNet [20].

Full-supervised node classification. For the full-supervised node classification, we compare GPNet with 18 baselines, including (1) MLP; (2) classical GNNs: GCN [1], GAT [2], SGC [23], MixHop [3], and APPNP [18]; (3) GNNs for heterophily settings: (4) Geom-GCN [45], H₂GCN [53], FAGCN [46], LINKX [54], GPRGNN [48], and GGCN [55]; (5) deep GNNs: GCNII [22] and DeepGCNs [56]; (6) recent SOTA GNNs: UDGNN_{GCN} [57], Conn-NSD [58], GloGNN [59], and GloGNN++ [59].

Inductive learning. For the large graph Reddit, several general models that target large graphs are listed as baselines: SAGE-GCN [32], SAGE-LSTM [32], SAGE-mean [32], FastGCN [9],

GaAN [37], and DGI [60]. In addition, on the large graph, we also compare our method with recent SOTA GNNs, including GCN [1], GAT [2], SGC [23], GCNII [22], and GPRGNN [48].

5.4 Results

Results for semi-supervised node classification. Table 2 summarizes the performance of GPNet to these SOTA baselines on the semi-supervised node classification tasks. We have these findings: (1) SGC that removes the activation function achieves similar performance to GCN model, which suggests that non-linear functions are not necessary to improve the results. (2) High-order GNNs such as MixHop-learn and APPNP improve the expressive power of GCN with one-order. (3) Deep GNNs such as GCNII outperform GCN by significant margins. This shows that these techniques of deep GNNs can effectively address the over-smoothing of multi-layer GCN. (4) Instead of stacking network layers, GPNet, obtains the SOTA performance in terms of average rank and average accuracy among all baselines on Pubmed, Citeseer, and Cora, using the geometric polynomials of adjacency matrices with various dilation factors, improves over GCN by 3.2%, 6.4%, and 3.8%, improves over SGC by 3.3%, 4.0%, and 4.4%, and improves over FAGCN by 2.6%, 2.9%, and 0.6%, respectively. These results provide positive answers to question Q1.

Results for full-supervised node classification. To support answering Q2 and Q4, we compare GPNet with these SOTA node classification baselines on the full-supervised node classification tasks, and the results are summarized in Table 3. From the table, we make the following observations: (1) MLP that uses only node’s own feature performs surprisingly well on webpage networks (Wisconsin, Cornell, and Texas), but achieves poor performance on these networks with a medium-scale number of nodes and edges (Wikipedia networks and citation networks). This shows the importance of node’s own feature to small-scale graphs. (2) GCNII with the initial residual and identity mapping significantly outperforms that of GCN, GAT, and SGC, and achieves best performance with homophily graphs. This shows that the initial residual and identity mapping mechanisms effectively address the over-smoothing of classical GNN models. (3) Overall, GNNs

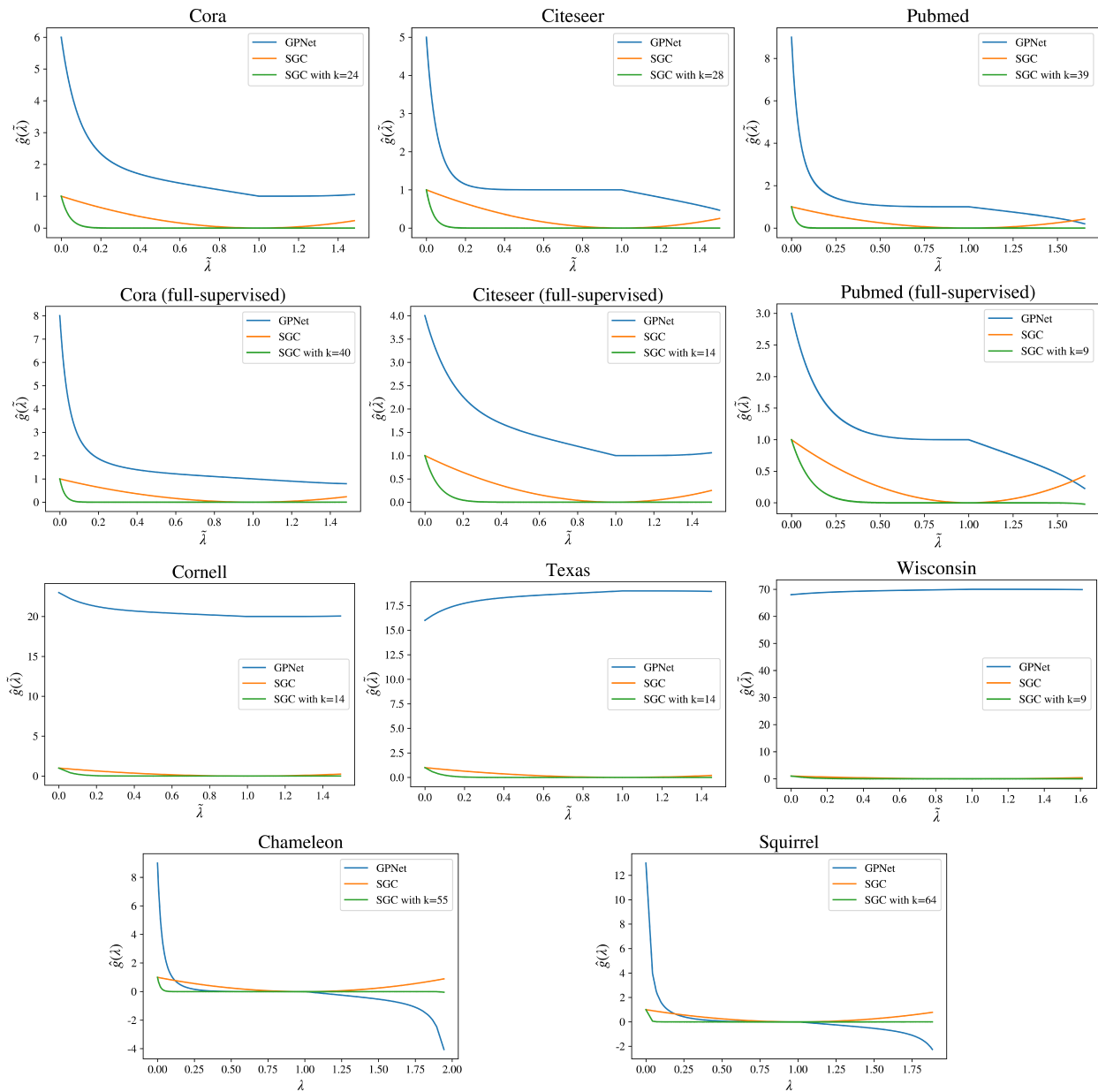


Fig. 3. **Filters learnt on graph datasets by GPNNet and SGC.** $\lambda/\tilde{\lambda}$ are the eigenvalues with / without self-loops, and $\hat{g}(\tilde{\lambda})/\hat{g}(\lambda)$ are the corresponding filter coefficients.

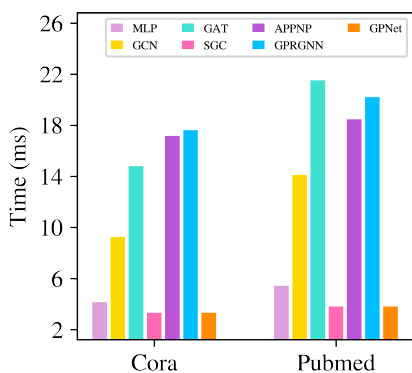


Fig. 4. **Performance over average training time per epoch on Cora and Pubmed.**

with heterophily settings achieve superior results on heterophily datasets. For example, on Chameleon, Squirrel, Wisconsin, Cornell, and Texas datasets, the accuracy scores of GGCN are 71.14%, 55.17%, 86.86%, 85.68%, and 84.86%, respectively. These results provide strong support for the techniques used on heterophily datasets. (4) We observe that GPNNet achieves new SOTA performance in terms of average rank and average accuracy over all the datasets. This demonstrates the effectiveness of the proposed model to performance improvement on both homophily and heterophily datasets.

Results for inductive learning. Table 4 shows the results of GPNNet and competing methods on Reddit. On Reddit, we observe that GPNNet ranks second and the GNNs such as GAT fail to run. These results provide positive answers to question Q3.

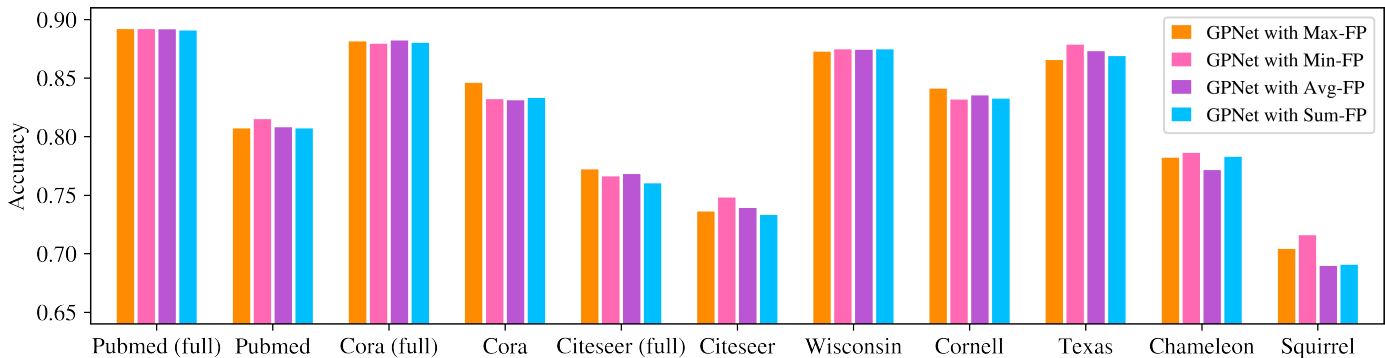


Fig. 5. Performance of GPNet with different aggregation functions on both homophily and heterophily datasets.

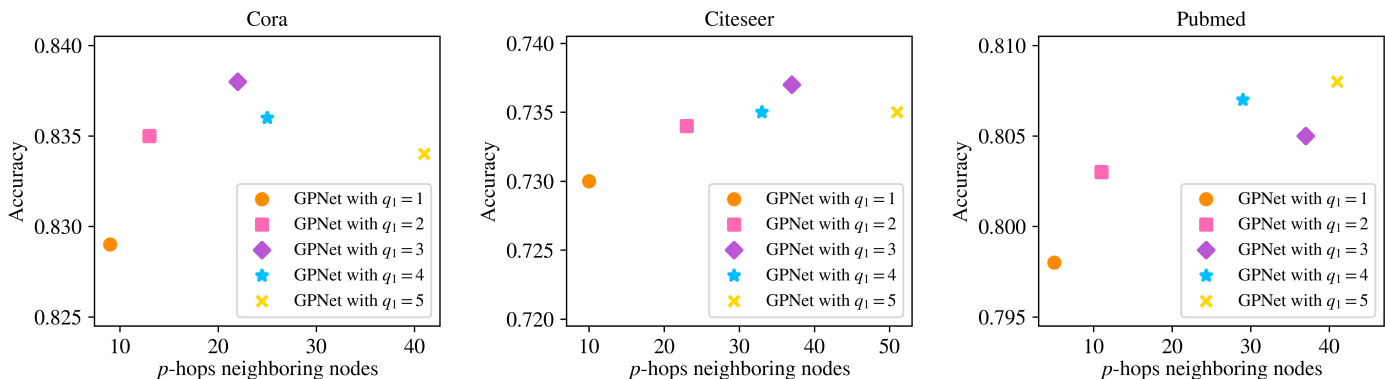


Fig. 6. Effect of GPNet with various dilation factors (q_1). x -axis denotes the p -hops neighboring nodes captured by the respective models to achieve the best performance.

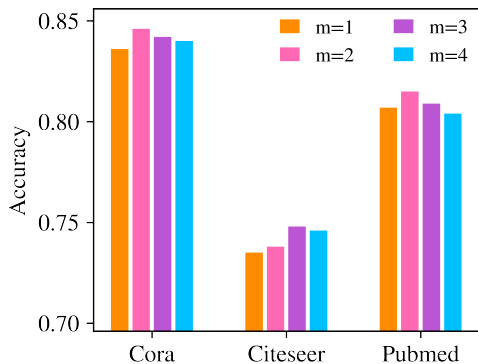


Fig. 7. Effect of channels (m).

5.5 Learning of Filters

Figure 3 depicts the filters learnt by GPNet and SGC on different datasets. On all datasets, SGC retains the low-frequency signals of node features while filtering out the high-frequency signals of node features. However, the high-frequency signals are helpful for heterophily graphs [46]. Therefore, SGC is optimal for homophily datasets but fails to work well on heterophily datasets. Figure 3 shows that SGC with $k = 24$ model suffers from the over-smoothing and almost ignores all node features on Cora. GPNet pays attention to signals of different frequencies according to different graph statistics (homophily ratio, nodes, and edges). In GPNet, we mainly consider the low-frequency signals while

paying less attention to the high frequency signals on homophily datasets. In addition, on Cornell, Texas, and Wisconsin datasets with heterophily and small-scale nodes and edges, GPNet captures both the low-frequency and high-frequency signals. On other heterophily datasets, GPNet mainly considers the high-frequency signals.

5.6 Analysis of Efficiency and Parameters

Figure 4 lists the performance of MLP and the representative GNNs over their training time per epoch relative to that of GPNet on Cora and Pubmed datasets. In Figure 4, in terms of training time per epoch, GPNet achieves as good performance as SGC, and takes fewer computations compared to other baselines. The larger datasets see the most benefit. For example, on Pubmed, compared with GCN, GPNet achieves a 73.0% speed up. As shown in Section 4.4, we can precompute the parameter-free feature extraction \bar{H} in the same way as SGC. Then GPNet and SGC only learn a single weight matrix during training. This indicates that both of them can consistently provide fewer computations and parameters, which provides positive answers to question Q5.

5.7 Ablation Study

Effect of Aggregation function. We conduct the experiments using the proposed aggregation functions on both homophily and heterophily datasets. The results are summarized in Figure 5. The best performance on different datasets varies slightly for GPNet models with different aggregation functions. Specifically, GPNet

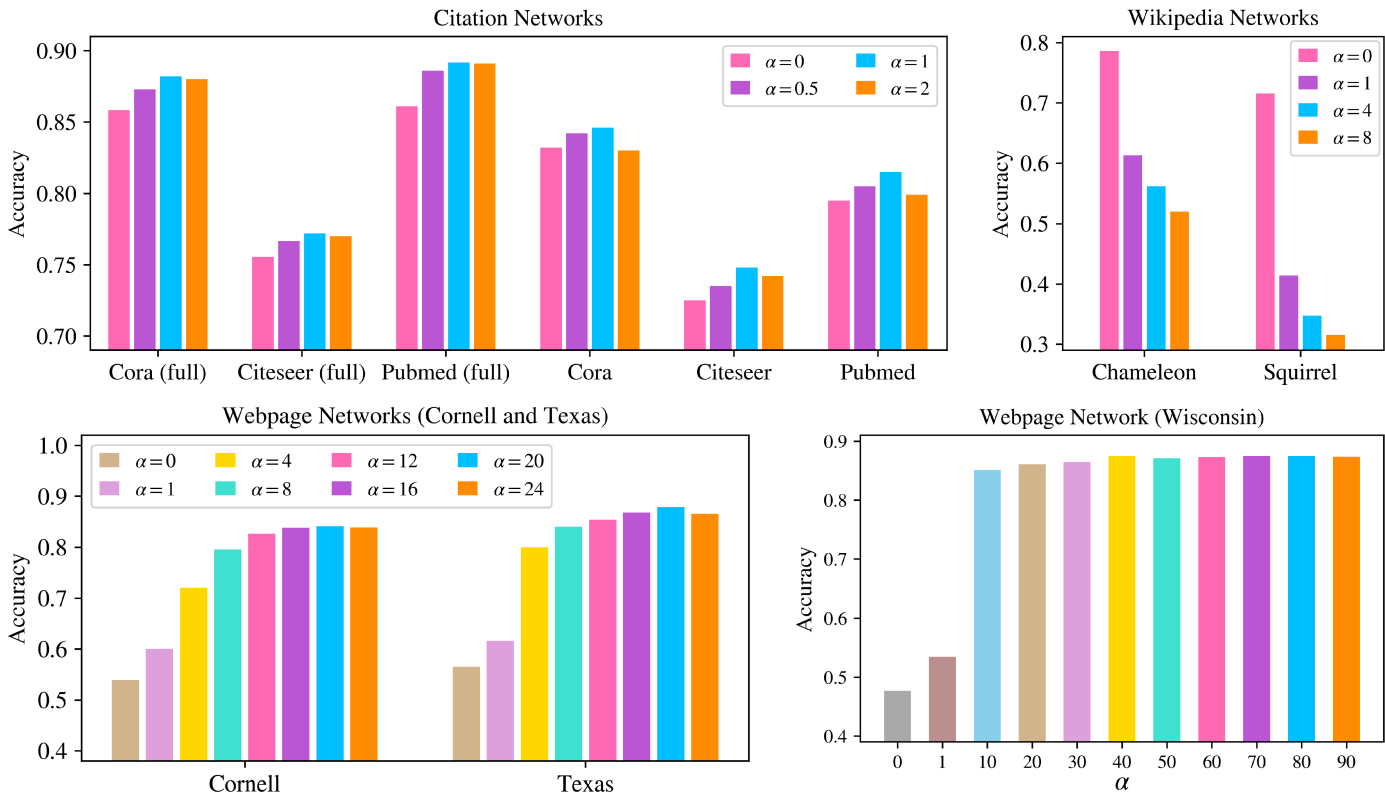


Fig. 8. **Effect of self-attention score** (α). Citation networks are homophily networks, and other networks are heterophily networks.

with Max-FP achieves the highest test accuracy on Cora, Citeseer (full), and Cornell datasets, GPNet with Min-FP achieves the best results on Pubmed (full), Pubmed, Citeseer, Texas, Chameleon, and Squirrel datasets, GPNet with Avg-FP obtains the highest classification accuracy on Cora (full) dataset, and GPNet with Sum-FP obtains the best performance on Wisconsin dataset.

Effect of dilation. We take GPNet with $m = 1$ as an example, repeatedly optimize the number of terms of the geometric polynomial using different dilation factors to achieve the best test accuracy for the respective models. The results are summarized in Figure 6. We observe that GPNet models with $q_1 > 1$ can capture the features of neighboring nodes at more distant distances and achieve better performance, compared to GPNet with $q_1 = 1$.

Effect of channel. Figure 7 compares the performance of GPNet models with different channels. From the results, we observe that GPNet models with $m=2$ and 3 outperform GPNet with $m=1$ by a large margin. This shows that multiple channels contribute to the performance improvement.

Effect of self-attention score. Figure 8 shows the comparison results of the proposed models with various self-attention scores for different types of networks. From the figure, we make the following observations: (1) On the citation networks, the accuracy of GPNet improves as the self-attention score increases (increases α) until α of 1. By further increasing α , the accuracy of GPNet begins to decrease. (2) On the medium-scale Wikipedia networks, GPNet with $\alpha = 0$ achieves the best performance, and the performance of the model decreases as α increases. (3) On the small-scale webpage networks, GPNet with $\alpha = 20$ outperforms other methods on Cornell and Texas, and GPNet with $\alpha = 40$ and GPNet with $\alpha = 70$ are better than other methods. These

observations imply that self-nodes and neighboring nodes that are p -hops away play an equally important role in training homophily networks, self-nodes are harmful for performance improvement on medium-scale heterophily networks, and self-nodes are particularly important in training small-scale heterophily networks compared to the neighboring nodes.

Effect of sign factor and filter. Figure 9 summarizes the performance of various sign factors. We observe that different sign factors help performance in training different types of networks. Notably, we find that their models achieve the same performance when the graph filters are symmetric to each other about the x -axis. This shows that the performance depends on the non-zero part of the spectral coefficients, regardless of the filter type. This theoretical explanation can be found in Section 4.1.

Effect of terms. Figure 10 depicts the validation results achieved by varying the number of terms $k \in 1..9$ of different channels. We see that the overall accuracy of the proposed models with different channels tends to improve as k increases. Compared with GPNet with $m=1$, GPNet with $m=2$ attains higher performance across various terms. The results further support the design of multi-channel learning.

Effect of adjacency matrix. We investigate the effect of whether adjacency matrix has self-loops. As shown in Table 5, GPNet with \hat{A} (adjacency matrix with self-loops) consistently works better on these datasets with small average degree while performing slightly worse on other datasets compared to GPNet without \hat{A} . This study demonstrates that adjacency matrix with self-loops is suitable for graphs with small average degree, while adjacency matrix without self-loops contributes to the performance of graphs with large average degree.

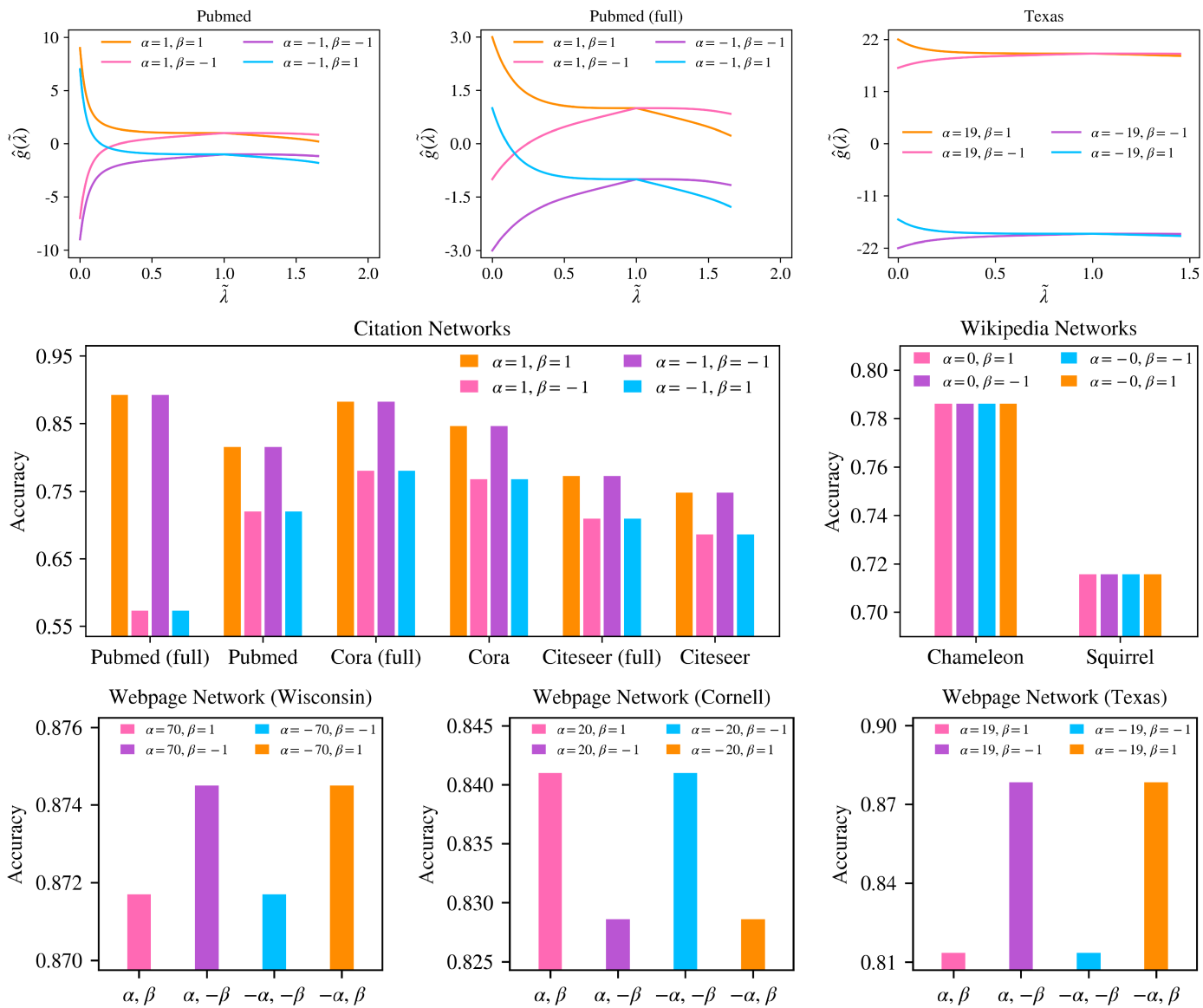


Fig. 9. **Effect of sign factor (β) and filter.** Citation networks are homophily networks, and other networks are heterophily networks.

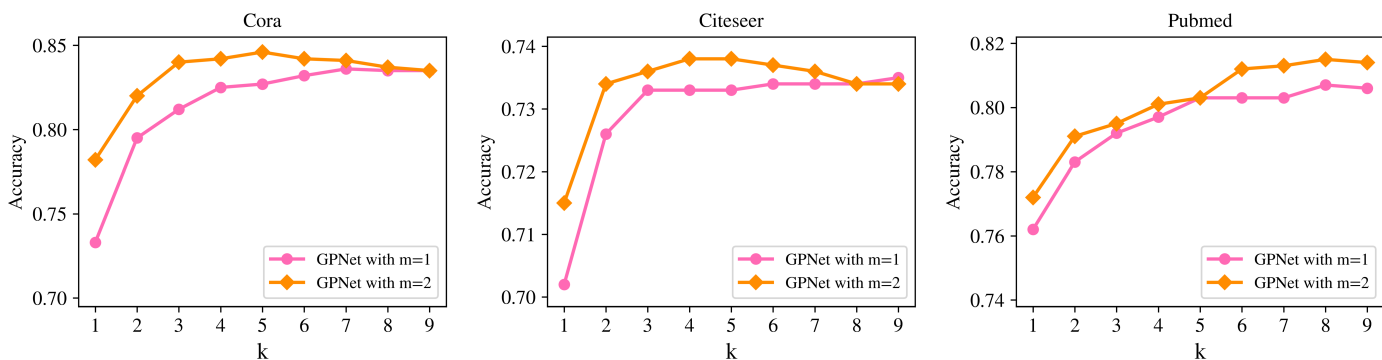


Fig. 10. **Effect of terms (k).**

Effect of ReLU. Table 6 shows the effect of whether GPNet has ReLU on all datasets. We see that GPNet without ReLU attains higher accuracy and more stable performance compared to GPNet

with ReLU. This may be because the activation function destroys the captured feature information. Therefore, we propose to remove the nonlinear activation function in the design of GNNs.

TABLE 6
Effect of GPNet with / without ReLU. GPNet-ReLU is GPNet with ReLU.

Method	Chameleon	Squirrel	Wisconsin	Cornell	Texas	Pubmed (full)	Citeseer (full)	Cora (full)	Pubmed	Citeseer	Cora
GPNet-ReLU	60.56±4.1	31.44±5.0	83.41±3.1	82.04±1.4	86.41±0.5	86.33±1.8	75.56±1.2	78.53±2.1	72.2±11.0	74.3±0.1	84.4±0.1
GPNet (ours)	78.61±0.2	71.57±0.1	87.45±0.0	84.10±0.1	87.84±0.0	89.18±0.0	77.20±0.1	88.21±0.1	81.5±0.0	74.8±0.1	84.6±0.1

TABLE 5
Effect of adjacency matrix with / without self-loops. The average degree is equal to 2 times the number of edges divided by the number of nodes, and A. M. and SL are Adjacency Matrix and Self-loops, respectively.

Dataset	Average Degree	A. M. with SL	A. M. without SL
Cora	4.01	84.6 ± 0.1	83.7 ± 0.4
Citeseer	2.84	74.8 ± 0.1	73.2 ± 0.2
Pubmed	4.50	81.5 ± 0.0	80.0 ± 0.0
Cora (full)	4.01	88.21 ± 0.1	87.80 ± 0.0
Citeseer (full)	2.84	77.20 ± 0.1	76.46 ± 0.1
Pubmed (full)	4.50	89.18 ± 0.0	88.92 ± 0.0
Chameleon	31.71	71.03 ± 0.1	78.61 ± 0.2
Squirrel	76.14	63.33 ± 0.1	71.57 ± 0.1
Wisconsin	3.98	87.45 ± 0.0	87.10 ± 0.1
Cornell	3.22	84.10 ± 0.1	83.35 ± 0.1
Texas	3.38	87.84 ± 0.0	84.86 ± 0.0

6 CONCLUSION

In this paper, to address the limitations of existing GNNs, we have investigated the proposed designs that improve the expressive power of learning graph representations. With the designs, we design the GPNet model that learns a distribution under optimal efficiency and parameters by precomputing the fixed feature extraction on both heterophily and homophily networks. We theoretically analyze that the model can correspond to different types of filters. Experiments on various graph learning tasks show that the model achieves significant performance gains over the state-of-the-art methods. For future work, an interesting direction is to apply the proposed model to directed networks.

ACKNOWLEDGMENTS

This research was funded by the National Natural Science Foundation of China (Grant No. 42274016/D0402, U1701266), the Program for Guangdong Introducing Innovative and Entrepreneurial Teams (Grant No.2019ZT08L213), the Natural Science Foundation of Guangdong Province (Grant No.2021A1515011483, 2022A1515011146), the Guangdong Provincial Key Laboratory of Intellectual Property and Big Data (Grant No. 2018B030322016), and Special Projects for Key Fields in Higher Education of Guangdong, China (Grant No. 2020ZDZX3077,2021ZDZX1042).

REFERENCES

- [1] TN Kipf and M. Welling, "Semi-supervised classification with graph convolutional networks," in *ICLR*, 2017, pp. 1–14.
- [2] P. Veličković, G. Cucurull, A. Casanova, A. Romero, P. Lio, and Y. Bengio, "Graph attention networks," in *ICLR*, 2018, pp. 1–12.
- [3] S. Abu-El-Haija, B. Perozzi, A. Kapoor, H. Harutyunyan, N. Alipourfard, K. Lerman, GV Steeg, and A. Galstyan, "MixHop: Higher-Order Graph Convolution Architectures via Sparsified Neighborhood Mixing," in *ICML*, 2019, pp. 21–29.
- [4] Y. Li, R. Yu, C. Shahabi, and Y. Liu, "Diffusion Convolutional Recurrent Neural Network: Data-Driven Traffic Forecasting," in *ICLR*, 2018.
- [5] Z. Cui, K. Henrickson, R. Ke, and Y. Wang, "Traffic graph convolutional recurrent neural network: A deep learning framework for network-scale traffic learning and forecasting," *IEEE Transactions on Intelligent Transportation Systems*, vol. 21, pp. 4883–4894, 2020.
- [6] T. Bogaerts, AD Masegosa, JS Onieva, E. Onieva, and P. Hellinckx, "A graph CNN-LSTM neural network for short and long-term traffic forecasting based on trajectory data," *Transportation Research Part C: Emerging Technologies*, vol. 112, pp. 62–77, 2020.
- [7] L. Chen, L. Wu, R. Hong, K. Zhang, and M. Wang, "Revisiting Graph Based Collaborative Filtering: A Linear Residual Graph Convolutional Network Approach," in *AAAI*, 2020, pp. 27–34.
- [8] Wenhui Yu, and Zheng Qin, "Graph Convolutional Network for Recommendation with Low-pass Collaborative Filters," in *ICML*, 2020, pp. 10936–10945.
- [9] J. Chen, T. Ma, and C. Xiao, "FastGCN: Fast Learning with Graph Convolutional Networks via Importance Sampling," in *ICLR*, 2018.
- [10] P. Tong, Q. Zhang, J. Yao, "Leveraging Domain Context for Question Answering Over Knowledge Graph," *Data Science and Engineering*, vol. 4, pp. 323–335, 2020.
- [11] A. Fout, J. Byrd, B. Shariat, and A. Ben-Hur, "Protein Interface Prediction using Graph Convolutional Networks," in *NeurIPS*, 2017, pp. 6530–6539.
- [12] J. Shang, C. Xiao, T. Ma, H. Li, and J. Sun, "GAMENet: Graph Augmented MEMory Networks for Recommending Medication Combination," in *AAAI*, 2019, pp. 1126–1133.
- [13] PC Rathi, RF Ludlow, and ML Verdonk, "Practical high-quality electrostatic potential surfaces for drug discovery using a graph-convolutional deep neural network," *Journal of medicinal chemistry*, vol. 63, pp. 8778–8790, 2019.
- [14] D. Jiang, Z. Wu, C. Hsieh, G. Chen, B. Liao, Z. Wang, C. Shen, D. Cao, J. Wu, and T. Hou, "Could graph neural networks learn better molecular representation for drug discovery? A comparison study of descriptor-based and graph-based models," *Journal of Cheminformatics*, vol. 13, pp. 1–23, 2021.
- [15] Z. Chen, X. Wei, P. Wang, and Y. Guo, "Multi-Label Image Recognition With Graph Convolutional Networks," in *CVPR*, 2019, pp. 5177–5186.
- [16] L. Zhao, X. Peng, Y. Tian, M. Kapadia, and DN Metaxas, "Semantic Graph Convolutional Networks for 3D Human Pose Regression," in *CVPR*, 2019, pp. 3425–3435.
- [17] Q. Li, Z. Han, and X. Wu, "Deeper Insights into Graph Convolutional Networks for Semi-Supervised Learning," in *AAAI*, 2018, pp. 3538–3545.
- [18] J. Klicpera, A. Bojchevski, and S. Günnemann, "Predict then Propagate: Graph Neural Networks meet Personalized PageRank," in *ICLR*, 2019.
- [19] K. He, X. Zhang, S. Ren, and J. Sun, "Deep residual learning for image recognition," in *CVPR*, 2016, pp. 770–778.
- [20] K. Xu, C. Li, Y. Tian, T. Sonobe, K. Kawarabayashi, and S. Jegelka, "Representation Learning on Graphs with Jumping Knowledge Networks," in *ICML*, 2016, pp. 5449–5458.
- [21] Y. Rong, W. Huang, T. Xu, and J. Huang, "DropEdge: Towards Deep Graph Convolutional Networks on Node Classification," in *ICLR*, 2020.
- [22] M. Chen, Z. Wei, Z. Huang, B. Ding, and Y. Li, "Simple and Deep Graph Convolutional Networks," in *ICML*, 2020, pp. 1725–1735.
- [23] F. Wu, AH Souza Jr., T. Zhang, C. Fifty, T. Yu, and KQ Weinberger, "Simplifying Graph Convolutional Networks," in *ICML*, 2019, pp. 6861–6871.
- [24] J. Zhu, Y. Yan, L. Zhao, M. Heimann, L. Akoglu, and D. Koutra, "Beyond homophily in graph neural networks: Current limitations and effective designs," in *NeurIPS*, 2020, pp. 7793–7804.
- [25] J. Zhu, RA Rossi, A. Rao, T. Mai, N. Lipka, NK Ahmed, and D. Koutra, "Graph neural networks with heterophily," in *AAAI*, 2021, pp. 11168–11176.
- [26] X. Liu, F. Lei, G. Xia, Y. Zhang, and W. Wei, "AdjMix: simplifying and attending graph convolutional networks," *Complex & Intelligent Systems*, vol. 8, pp. 1005–1014, 2022.
- [27] F. Yu and V. Koltun, "Multi-scale context aggregation by dilated convolutions," in *ICLR*, 2016.
- [28] J. Bruna, W. Zaremba, A. Szlam, and Y. LeCun, "Spectral networks and locally connected networks on graphs," in *ICLR*, 2014, pp. 1–14.

- [29] M. Defferrard, X. Bresson, and P. Vandergheynst, “Convolutional Neural Networks on Graphs with Fast Localized Spectral Filtering,” in *NeurIPS*, 2016, pp. 3837–3845.
- [30] J. Zhou, G. Cui, S. Hu, Z. Zhang, C. Yang, Z. Liu, L. Wang, C. Li, and M. Sun, “Graph neural networks: A review of methods and applications,” *AI Open*, vol. 1, pp. 57–81, 2020.
- [31] G. Li, M. Müller, AK Thabet, and B. Ghanem, “DeepGCNs: Can GCNs Go As Deep As CNNs?,” in *ICCV*, 2019, pp. 9266–9275.
- [32] WL Hamilton, Z. Ying, and J. Leskovec, “Inductive Representation Learning on Large Graphs,” in *NeurIPS*, 2017, pp. 1024–1034.
- [33] W. Huang, T. Zhang, Y. Rong, and J. Huang, “Adaptive Sampling Towards Fast Graph Representation Learning,” in *NeurIPS*, 2018, pp. 4563–4572.
- [34] W. Chiang, X. Liu, S. Si, Y. Li, S. Bengio, and C. Hsieh, “ClusterGCN: An Efficient Algorithm for Training Deep and Large Graph Convolutional Networks,” in *KDD*, 2019, pp. 257–266.
- [35] KK Thekumparampil, C. Wang, S. Oh, and LJ Li, “Attention-based graph neural network for semi-supervised learning,” *arXiv preprint arXiv:1803.03735*, 2018.
- [36] M. Kampffmeyer, Y. Chen, X. Liang, H. Wang, Y. Zhang, and EP Xing, “Rethinking Knowledge Graph Propagation for Zero-Shot Learning,” in *CVPR*, 2019, pp. 11487–11496.
- [37] J. Zhang, X. Shi, J. Xie, H. Ma, I. King, and D. Yeung, “Gaan: Gated attention networks for learning on large and spatiotemporal graphs,” in *UAI*, 2018, pp. 339–349.
- [38] JB Lee, RA Rossi, S. Kim, NK Ahmed, and E. Koh, “Attention Models in Graphs: A Survey,” *ACM Transactions on Knowledge Discovery from Data*, vol. 13, pp. 62:1–62:25, 2019.
- [39] S. Abu-El-Haija, A. Kapoor, B. Perozzi, and J. Lee, “N-GCN: Multi-scale graph convolution for semi-supervised node classification,” in *UAI*, 2019, pp. 841–851.
- [40] R. Liao, Z. Zhao, R. Urtasun, and RS Zemel, “LanczosNet: Multi-Scale Deep Graph Convolutional Networks,” in *ICLR*, 2019, pp. 1–18.
- [41] S. Luan, M. Zhao, X. Chang, and D. Precup, “Break the Ceiling: Stronger Multi-scale Deep Graph Convolutional Networks,” in *NeurIPS*, 2019, pp. 10943–10953.
- [42] F. Lei, X. Liu, Q. Dai, BW Ling, H. Zhao, and Y. Liu, “Hybrid Low-Order and Higher-Order Graph Convolutional Networks,” *Computational Intelligence and Neuroscience*, vol. 2020, pp. 3283890:1–3283890:9, 2020.
- [43] FM Bianchi, D. Grattarola, L. Livi, and C. Alippi, “Graph Neural Networks With Convolutional ARMA Filters,” *IEEE Transactions on Pattern Analysis and Machine Intelligence*, vol. 44, pp. 3496–3507, 2022.
- [44] H. NT and T. Maehara, “Revisiting Graph Neural Networks: All We Have is Low-Pass Filters,” *arXiv preprint arXiv:1905.09550*, 2019.
- [45] H. Pei, B. Wei, KC Chang, Y. Lei, B. Yang, “Geom-gcn: Geometric graph convolutional networks,” in *ICLR*, 2020.
- [46] D. Bo, X. Wang, C. Shi, and H. Shen, “Beyond Low-frequency Information in Graph Convolutional Networks,” in *AAAI*, 2021, pp. 3950–3957.
- [47] Y. Wang and T. Derr, “Tree decomposed graph neural network,” in *CIKM*, 2021, pp. 2040–2049.
- [48] E. Chien, J. Peng, P. Li, and O. Milenkovic, “Adaptive universal generalized pagerank graph neural network,” in *ICLR*, 2021.
- [49] P. Sen, G. Namata, M. Bilgic, L. Getoor, B. Galligher, and T. Eliassi-Rad, “Collective Classification in Network Data,” *AI magazine*, vol. 29, pp. 93–106, 2008.
- [50] B. Rozemberczki, C. Allen, and R. Sarkar, “Multi-scale attributed node embedding,” *Journal of Complex Networks*, vol. 9, 2021.
- [51] DP Kingma and J. Ba, “Adam: A Method for Stochastic Optimization,” in *ICLR*, 2015, pp. 1–15.
- [52] A. Paszke, S. Gross, F. Massa, A. Lerer, J. Bradbury, G. Chanan, T. Killeen, Z. Lin, N. Gimelshein, L. Antiga, A. Desmaison, A. Köpf, EZ Yang, Z. DeVito, M. Raison, A. Tejani, S. Chilamkurthy, B. Steiner, L. Fang, J. Bai, and S. Chintala, “PyTorch: An Imperative Style, High-Performance Deep Learning Library,” in *NeurIPS*, 2019, pp. 8024–8035.
- [53] J. Zhu, Y. Yan, L. Zhao, and M. Heimann, “Generalizing graph neural networks beyond homophily,” *arXiv preprint arXiv:2006.11468*, 2020.
- [54] D. Lim, F. Hohne, X. Li, SL Huang, V. Gupta, O. Bhalerao, and S. Lim, “Large Scale Learning on Non-Homophilous Graphs: New Benchmarks and Strong Simple Methods,” in *NeurIPS*, 2021, pp. 20887–20902.
- [55] Y. Yan, M. Hashemi, K. Swersky, Y. Yang, and D. Koutra, “Two sides of the same coin: Heterophily and oversmoothing in graph convolutional neural networks,” *arXiv preprint arXiv:2102.06462*, 2021.
- [56] G. Li, M. Müller, G. Qian, IC Delgadillo, A. Abualshour, A. Thabet, and B. Ghanem, “DeepGCNs: Making GCNs Go as Deep as CNNs,” *IEEE Transactions on Pattern Analysis and Machine Intelligence*, 2021.
- [57] J. Chen, W. Liu, Z. Huang, J. Gao, J. Zhang, and J. Pu, “Universal Deep GNNs: Rethinking Residual Connection in GNNs from a Path Decomposition Perspective for Preventing the Over-smoothing,” *arXiv preprint arXiv:2205.15127*, 2022.
- [58] F. Barbero, C. Bodnar, H. Borde, M. Bronstein, P. Veličković, and P. Liò, “Sheaf Neural Networks with Connection Laplacians,” *arXiv preprint arXiv:2206.08702*, 2022.
- [59] X. Li, R. Zhu, Y. Cheng, C. Shan, S. Luo, D. Li, and W. Qian, “Finding Global Homophily in Graph Neural Networks When Meeting Heterophily,” in *ICML*, 2022, pp. 13242–13256.
- [60] P. Veličković, W. Fedus, W. L. H., P. Liò, Y. Bengio, and RD Hjelm, “Deep Graph Infomax,” in *ICLR*, 2019, pp. 1–19.